Turbidity Current Hydrodynamics and Seabed Morphology

Marcelo H. García
Department of Civil and Environmental Engineering
University of Illinois at Urbana-Champaign
205 North Mathews Avenue
Urbana, Illinois 61801
phone: (217) 244-4484, fax: (217) 333-0687, email: mhgarcia@uiuc.edu

Award Number: N00014-93-1-0044
http://vtchl.uiuc.edu

LONG-TERM GOALS

Our main goal is to assess the hydrodynamics of turbidity currents and mudflows and their ability to produce morphological features such as ripples, dunes, antidunes and gullies along their paths. Of particular interest is to elucidate the role played by turbidity currents on the inception of submarine channels and canyons. To this end, understanding the mechanics of sediment erosion, including bedrock, by density currents is another long-term goal of this research.

OBJECTIVES

Our main objective is to advance our understanding of the seabed morphology associated with the passage of turbidity currents and mudflows. Different morphological features encountered in the marine environment are related to the action of bottom currents and turbidity currents. Large fields of long-wavelength, upslope-migrating bedforms observed on submarine channel levees are attributed to the action of unconfined turbidity currents that overflow channels and canyons and spread sediments across levees. Although it has been largely argued that such sediment waves, with ripples superimposed on them, are the result of downslope-flowing density underflows, the origin of such features still remains under debate.

APPROACH

Our approach consists of a combination of theoretical analysis, numerical modeling, and laboratory experiments. Stability analysis with multiple scales was used to investigate whether supercritical conservative density currents are capable of developing long-wavelength, upstream-migrating bedforms. Laboratory experiments were performed in the MARGINS TANK to observe if conservative density currents and depositional turbidity currents are capable of developing bedforms at different scales such as dunes and ripples, as well as long-wavelength, antidune-like, sediment waves. Two- and three-dimensional direct numerical simulations of a discontinuous density current propagating down a slope were conducted to assess the role of mixing on the flow dynamics.

WORK COMPLETED

A theoretical stability analysis has been completed using conservative density currents capable of transporting sediment as bedload as well as erosional turbidity currents. Comparison of maximum growth rate curves for the above mentioned cases, as function of Richardson number, show that

Report Documentation Page

Form Approved
OMB No. 0704-0188

1. REPORT DATE **30 SEP 2005**	2. REPORT TYPE	3. DATES COVERED **00-00-2005 to 00-00-2005**

4. TITLE AND SUBTITLE **Turbidity Current Hydrodynamics and Seabed Morphology**	5a. CONTRACT NUMBER
	5b. GRANT NUMBER
	5c. PROGRAM ELEMENT NUMBER
6. AUTHOR(S)	5d. PROJECT NUMBER
	5e. TASK NUMBER
	5f. WORK UNIT NUMBER
7. PERFORMING ORGANIZATION NAME(S) AND ADDRESS(ES) **University of Illinois at Urbana-Champaign,Department of Civil and Environmental Engineering,205 North Mathews Avenue, Urbana, , 61801**	8. PERFORMING ORGANIZATION REPORT NUMBER
9. SPONSORING/MONITORING AGENCY NAME(S) AND ADDRESS(ES)	10. SPONSOR/MONITOR'S ACRONYM(S)
	11. SPONSOR/MONITOR'S REPORT NUMBER(S)

12. DISTRIBUTION/AVAILABILITY STATEMENT
Approved for public release; distribution unlimited

13. SUPPLEMENTARY NOTES
code 1 only

14. ABSTRACT
Our main goal is to assess the hydrodynamics of turbidity currents and mudflows and their ability to produce morphological features such as ripples, dunes, antidunes and gullies along their paths. Of particular interest is to elucidate the role played by turbidity currents on the inception of submarine channels and canyons. To this end, understanding the mechanics of sediment erosion, including bedrock, by density currents is another long-term goal of this research.

15. SUBJECT TERMS

16. SECURITY CLASSIFICATION OF:			17. LIMITATION OF ABSTRACT	18. NUMBER OF PAGES	19a. NAME OF RESPONSIBLE PERSON
a. REPORT **unclassified**	b. ABSTRACT **unclassified**	c. THIS PAGE **unclassified**	**Same as Report (SAR)**	**13**	

Standard Form 298 (Rev. 8-98)
Prescribed by ANSI Std Z39-18

turbidity currents tend to form longer sediment waves than those associated with conservative density currents with bedload transport only. The analysis has been extended to account for the role played by the flow turbulence in the development of bedforms, by adding a conservation equation for turbulent kinetic energy.

More than thirty laboratory experiments were completed in the MARGINS TANK for: a) wide turbidity currents emanating from a line source and producing incipient gullies, and b) channelized turbidity currents generating a range of bedforms from ripples to dunes and antidunes.

Several two- and three-dimensional numerical simulations of discontinuous density currents were conducted. The numerical results were compared against unpublished laboratory observations previously made by the PI at the University of Minnesota. The numerical simulations were carried out using a stabilized, equal-order finite element method, in which a discontinuity-capturing technique was embedded for the salt transport. This technique captures sharp fronts with little spurious oscillations, allowing local features such as shear instabilities at density interfaces to be well reproduced.

RESULTS

Results obtained from the bed stability analysis indicate that both conservative and non-conservative supercritical dense underflows are able to develop long-sediment waves that migrate upslope, resembling antidunes (Fedele and Garcia, 2005a and 2005b). Figure 1 shows the components of the complex celerity of bed perturbations, as a function of wave-number (K), for a density current. In this figure, growth rate ($C_I > 0$) indicates that long sediment waves are likely to develop, whereas the celerity ($C_R < 0$) indicates an upstream migration for these bed instabilities. One of the important results obtained from the stability analysis is the spatial dependence of the (complex) dispersion relationship, which gives the growth rate of bed perturbations. Figure 2 shows growth rates of bed perturbations computed using the imaginary component of the dispersion relationship, for two different locations along the flow path. It is observed that antidunes formed by supercritical conservative density currents, with bedload transport only, tend to elongate, as the maximum growth rate moves towards smaller wavenumbers in the downslope direction. Also, the value of the positive peak of the growth rate tends to decrease in that direction as well, indicating that wave amplitude tends to decrease as the current flows downslope.

Laboratory experiments showed that conservative density currents and depositional turbidity currents are capable of developing bedforms at different scales such as dunes and ripples, as well as long-wavelength antidune-like sediment waves (Fedele, 2004). The laboratory observations in the MARGINS tank indicated that the front of turbidity currents plays an important on the bottom morphology. In particular, in order to be able to model the inception and development of gullies, it is necessary to have a 3-D hydrodynamic model of the flow.

NUMERICAL RESULTS

A rigorous model for two-way coupled multiphase flow has been developed. The model has been derived formally from the complete two-phase flow models presented in Zhang and Prosperetti (1997) and Balachandar and Ferry (2004). In contrast to the models presented by these authors, the model that we have developed is based on the volume-averaged velocity instead of the continuous phase velocity. In this way, by imposing the divergence-free condition to the velocity field, we satisfy exactly mass conservation since for incompressible phases mass conservation reduces to volume conservation. This feature of the model facilitates its implementation in standard incompressible Navier-Stokes solvers.

The derived momentum conservation equations present three terms in addition to the standard equations that account for the two-way coupling between phases. The model is completed by a transport equation for the void fraction, which is transported by the disperse phase velocity. For the disperse phase velocity we have derived a new version of the equilibrium Eulerian method based on the volume-averaged velocity. The derivation of the model was done by expanding all the terms using the small parameters τ and α (particle response time and volume fraction, respectively) and retaining terms $O(1)$, $O(\tau)$ and $O(\alpha)$, which makes the model exact to $O(\tau\alpha+\tau^2+\alpha^2)$. Finally, it is worth mentioning that the model is the most sophisticated version of the equilibrium Eulerian method: its innovations include exact multiphase volume conservation, finite settling velocity effects, and the incorporation of volume fraction gradient and Faxén terms. The derived model has been implemented in a spectral DNS channel flow code, which allows for the detailed resolution of fine-scale features without resorting to subscale modeling.

We have performed 3D simulations for planar and cylindrical configurations (Cantero et al. 2004a, Cantero et al. 2005c) with Gr=1.5 x 10^6 and Gr=1.5 x 10^7. The results are in figures 3 and 4. These solutions not only shows the Kevin-Helmholtz billows, but also the existence of a fast instability at the front of the current near the vertical boundaries that develops into a complex lobe and clef pattern. We can also observe the existence of an instability that develops at the interface of the current. Figure 5 shows the time evolution of the lobe and cleft instability. In this figure the front is visualized by contours of density. Figure 6 shows the radius of curvature of the front. Dark regions correspond to negative curvatures that are characteristic of clefts. Light color regions correspond to positive curvatures that are characteristic of lobes. Studies generalizing these results to particulate turbidity currents are under way (Cantero et al. 2005b).

We have also performed studies on the particles influence on the front velocity of gravity currents (Cantero et al. 2004b, Cantero et al. 2005a). Figure 7 shows the results for the limit when particles are so small that they act as a scalar field (τ =0 and w=0). The flow is visualized by a contour of dimensionless particle concentration =0.1. Soon after the release an intrusion front forms with a lifted nose due to the no-slip boundary condition. As the current advances, Kelvin-Helmholtz vortices are shed from the front which produce a net drag that balances the initial acceleration of the front. As a consequence, after the initial set-up of the Kelvin-Helmholtz vortices, the front moves at constant speed until the dilution in the current becomes important. Then, the current slows down and eventually dissipates.

Figures 8 and 9 show the results for currents of inertial particles with negligible settling (τ=0.05 and w=0 and τ =0.1 and w=0). Two contours are shown in these figures: the solid line contour that corresponds to particle concentration=0.1, and the dash line contour that corresponds to the initial particle concentration equal to 1. Two main differences are observed compared to the no-inertia-particles case. The first one is the migration of particles away from the core of the Kelvin-Helmholtz vortices, and the second one is the accumulation of particles in the front of the current, producing regions of particle concentration greater than the initial value. These two effects can be explained by noticing that the divergence of the particles velocity field is

$$\nabla \cdot \tilde{\mathbf{u}}_d = \tilde{\tau}(1-\beta)\left(\|\Omega\|^2 - \|\mathsf{S}\|^2\right)$$

where **S** and Ω are the symmetric and skew-symmetric parts of the local fluid velocity gradient tensor and β is the density ratio of the phases. Note from this equation that for particles substantially heavier than the continuous phase ($\beta = 0$), the divergence of the particle velocity field has the sign of ($||W||^2 - ||\mathbf{S}||^2$), which means that heavy particles migrate from regions of vorticity and accumulate in regions of high strain rate.

The preferential particles accumulation described above has a very important consequence in the current front velocity. Figure 10 shows the front velocity for the three different cases mentioned above. Observe that the front velocity in the phase of constant velocity increases for larger values of τ. The current with τ=0.1 presents a front velocity 5% larger that the current with τ=0.

IMPACT/APPLICATION

Theoretical analyses supported by laboratory observations have clearly shown the capability of turbidity currents for producing longitudinal small-scale bedforms such as ripples as well as long-wavelength antidunes. Our understanding of the mechanics of bedforms in continental margins until now has been rather limited and full of speculation. We hope that this work will facilitate both the interpretation of the geologic record as well as the design and placement of submarine structures on stable sediment deposits. Our work suggests that turbidity currents could also be a mechanism important for mine burial and should therefore receive more attention, particularly at river mouths where high-sediment discharges can generate such underflows.

RELATED PROJECTS

We are collaborating with Pat Wiberg, University of Virginia, and Lincoln Pratson, Duke University, to develop and incorporate a field-tested, mechanistic model for sediment erosion into our density current model as part of the EuroStrataform Program.

REFERENCES

S. Balachandar and J. Ferry, 2004.A simplified two-fluid model based on equilibrium closure for dilute dispersion of small particles. In preparation.

D. Zhang and A. Prosperetti, 1997. Momentum and energy equations for disperse two-phase flows and their closure for dilute suspensions. International Journal of Multiphase Flows, 23, 425-453.

Fedele J.J. and Garcia M.H. 2003. Bedforms and Density Underflows in the Marine Environment. *3rd IAHR Symposium on River, Coastal and Estuarine Morphodynamics*, , Barcelona, Spain, September.

Fedele, J.J., 2004. “Density Underflows and Bedforms in the Marine Environment,” Ph.D. Thesis, Department of Civil and Environmental Engineering, University of Illinois at Urbana-Champaign, October, 366p.

Parsons, J. and García, M., 1998. “Similarity of gravity current fronts”, *Physics of Fluids*, Vol. 10, Num. 12, pp. 3209-3213.

FY 2005 PUBLICATIONS

M. Cantero, S. Balachandar, and M. Garcia, 2005a. On the Front Velocity of Density Currents. *In preparation*.

M. Cantero, S. Balachandar, and M. Garcia, 2005b. Effect of Particle Inertia in Particulate Density Currents. In preparation.

M. Cantero, S. Balachandar, M. Garcia, and J. Ferry, 2005c. Direct numerical simulations of planar and cylindrical density currents. Accepted with revisions in the Journal of Applied Mechanics, ASME.

M. Cantero, J. Ferry, S. Balachandar, and M. Garcia, 2004a. Direct numerical simulations of axisymmetric density currents. Proceedings of the ENIEF, Bariloche, Argentina.

M. Cantero, S. Balachandar, M. Garcia and J. Ferry, 2004. Effect of particle inertia in particulate density currents. IUTAM Symposium on computational approaches to Disperse multiphase flow, Argonne, USA.

HONORS/AWARDS

Professor Marcelo Garcia has been elected Corresponding Member of the National Academy of Engineering of Argentina in the United States of America.

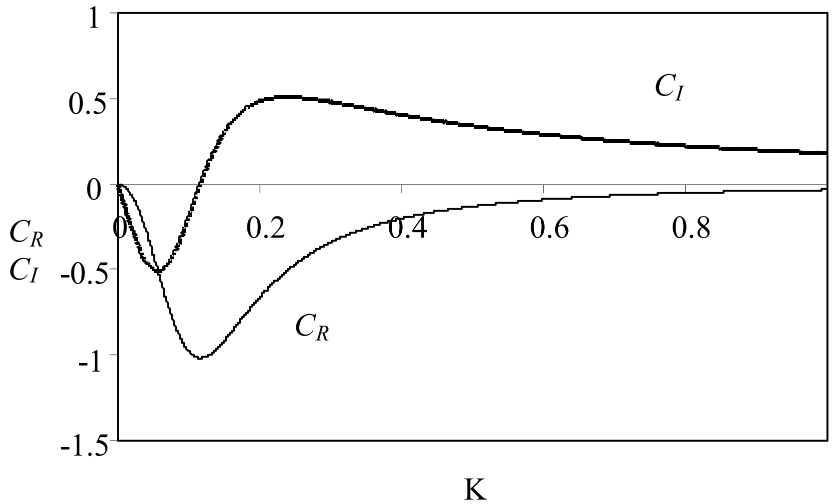

FIGURE 1. Stability of bed perturbations for a conservative density current with bedload transport. Figure shows imaginary and real components of the celerity of bed perturbations as functions of bedform wave number (x*=0).

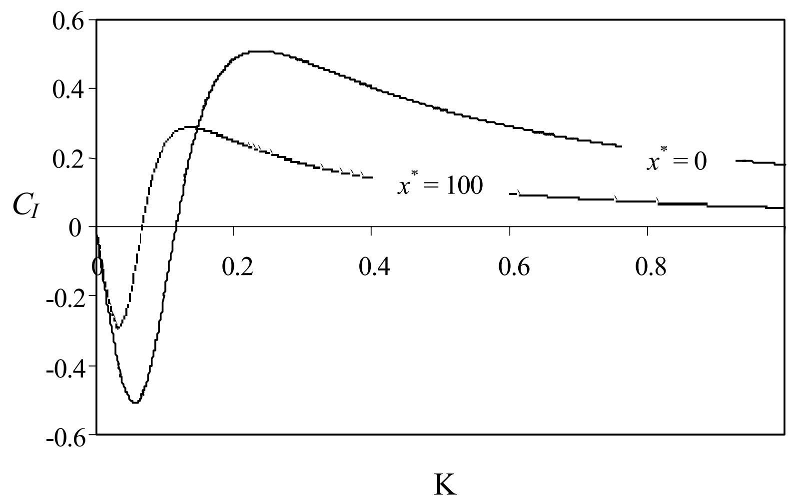

FIGURE 2. ***Down slope variation of characteristic wavelength and growth rate.***

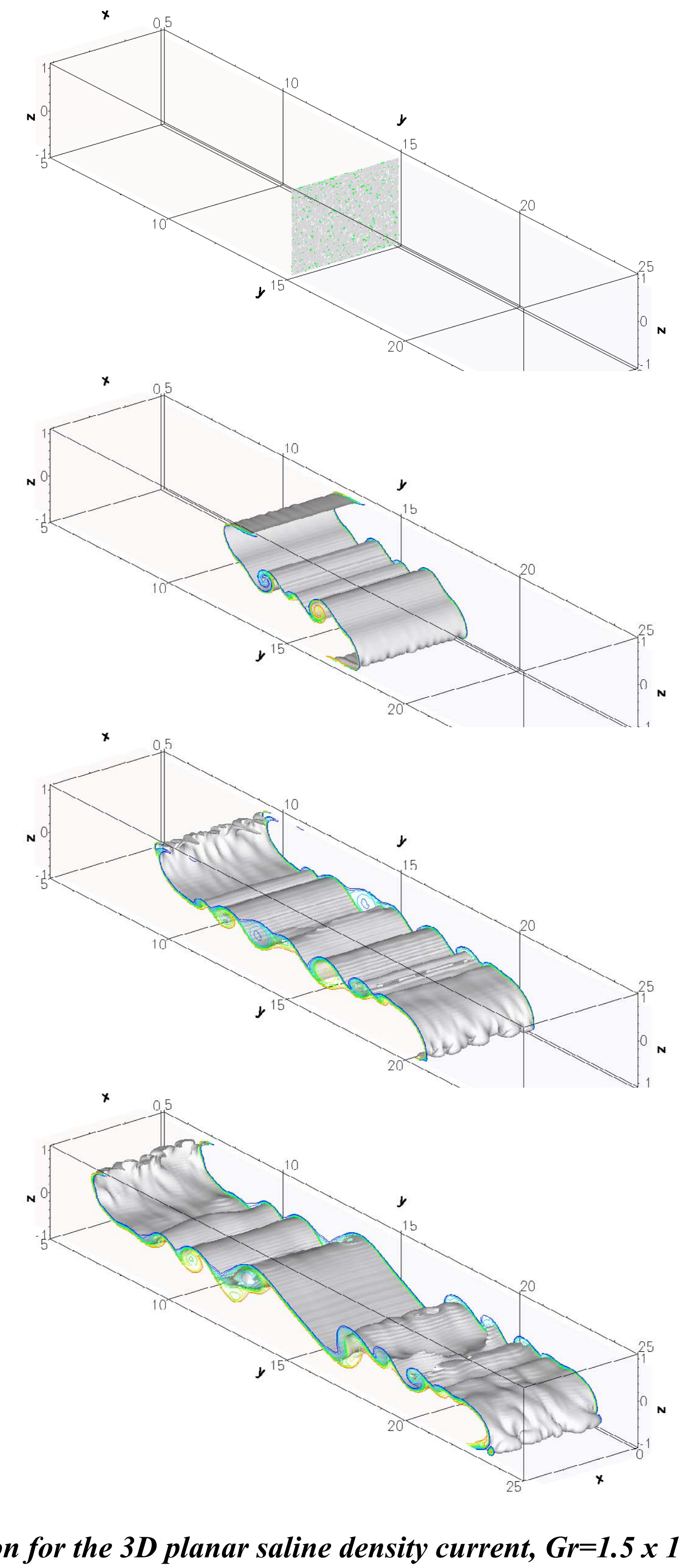

FIGURE 3. ***Solution for the 3D planar saline density current, Gr=1.5 x 10^{6}. From top to bottom t=0, t=5, t=10 and t=15. The surface represents a void fraction isosurface.***

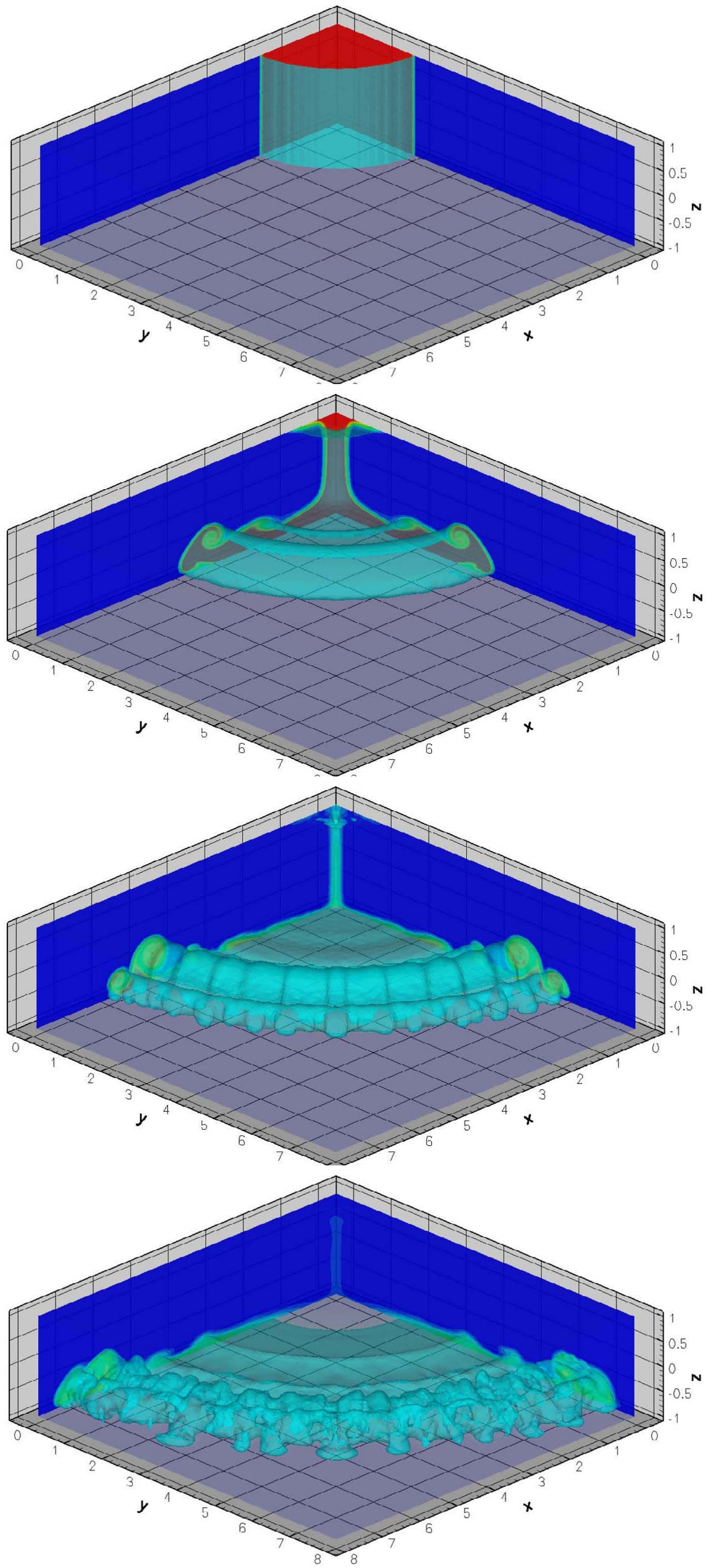

FIGURE 4. ***Solution for the 3D cylindric saline density current, Gr=1.5 x 10^6. From top to bottom t=0, t=4, t=8 and t=12. The surface represents a void fraction isosurface.***

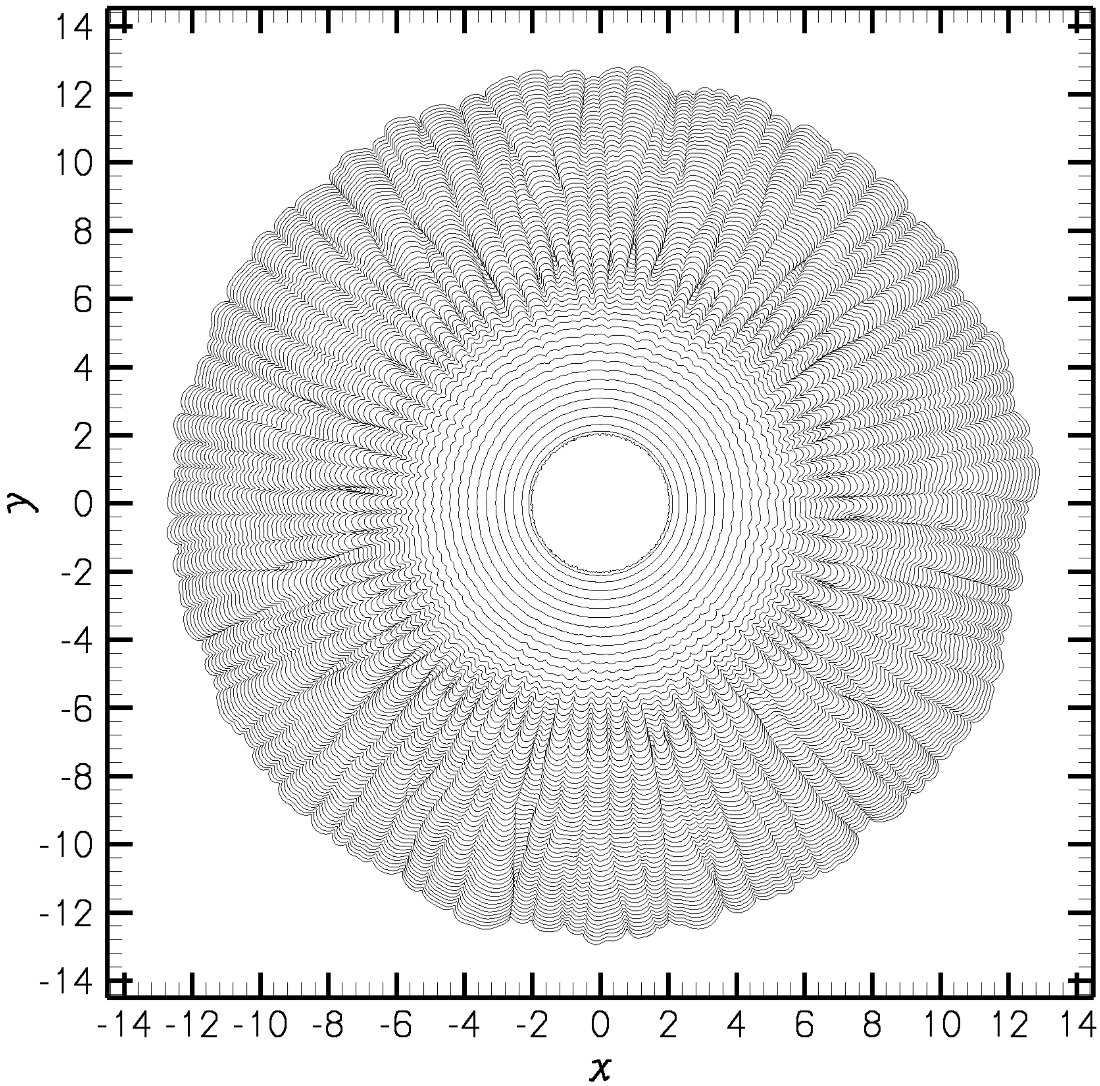

FIGURE 5. ***Time evolution of lobe and cleft instabilities visualized by density contours. Solution for the 3D cilindric saline density current, Gr=1.5 x 10^6.***

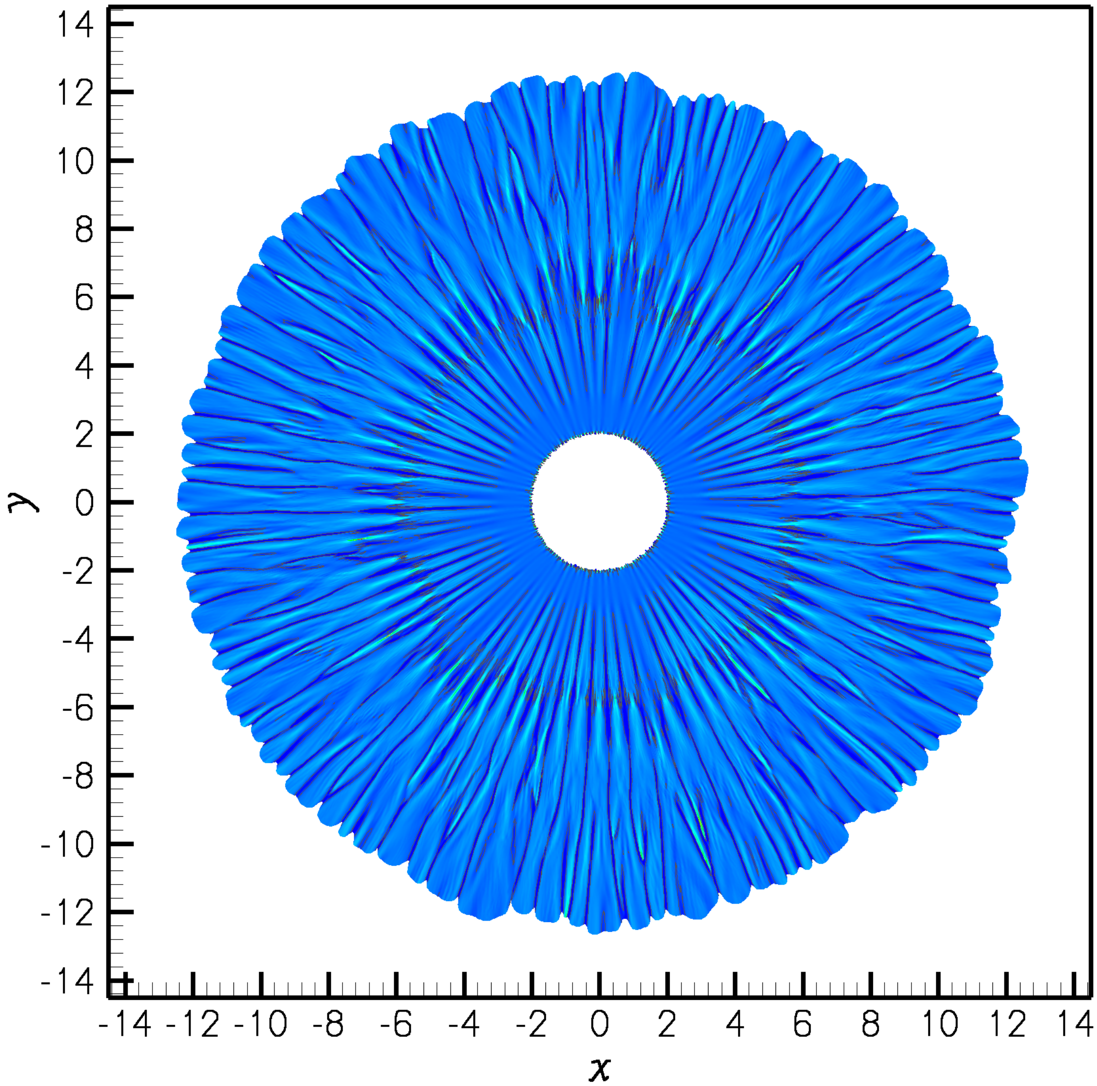

FIGURE 6. ***Time evolution of curvature of lobe and cleft instabilities. Solution for the 3D cylindrical saline density current, Gr=1.5 x 10⁶.***

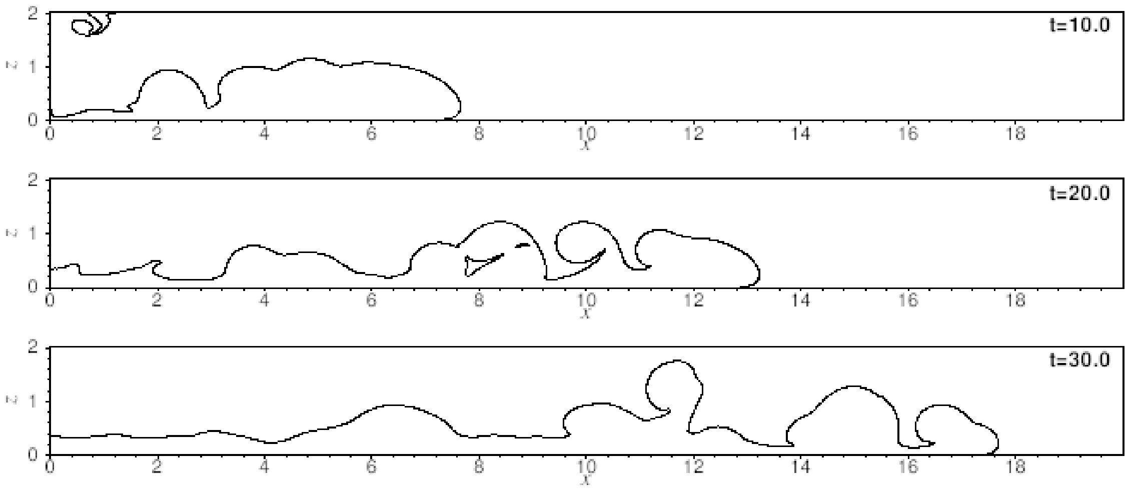

FIGURE 7. ***Contours of particle concentration, solid line= 0.1. Solution for τ=0 , w=0 and Gr=1.5 x 10^6.***

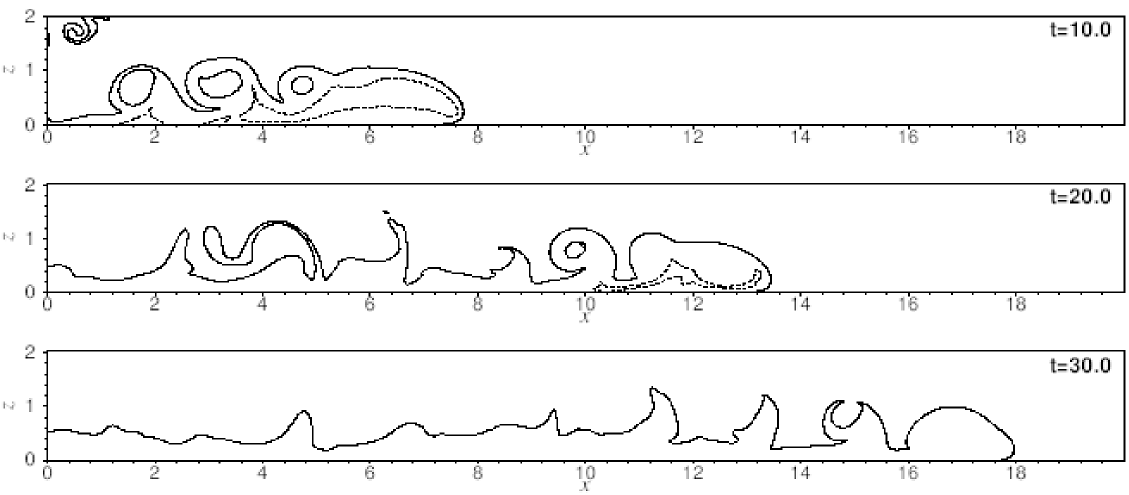

FIGURE 8. ***Contours of particle concentration, solid line= 0.1 and dash line =1.0. Solution for τ=0.05 , w=0 and Gr=1.5 x 10^6.***

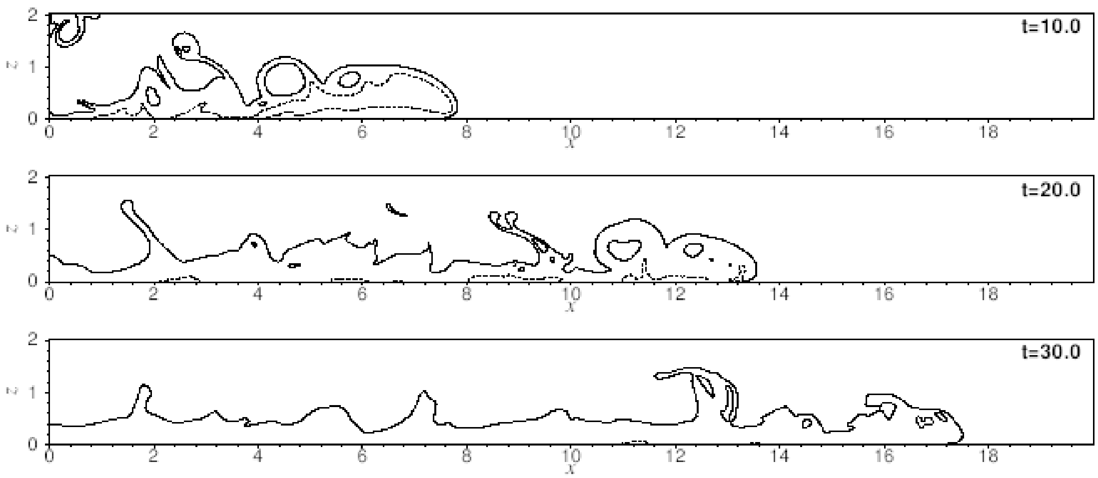

FIGURE 9. ***Contours of particle concentration solid line= 0.1 and dashed line=1.0. Solution for τ=0.1 , w=0 and Gr=1.5 x 10^6.***

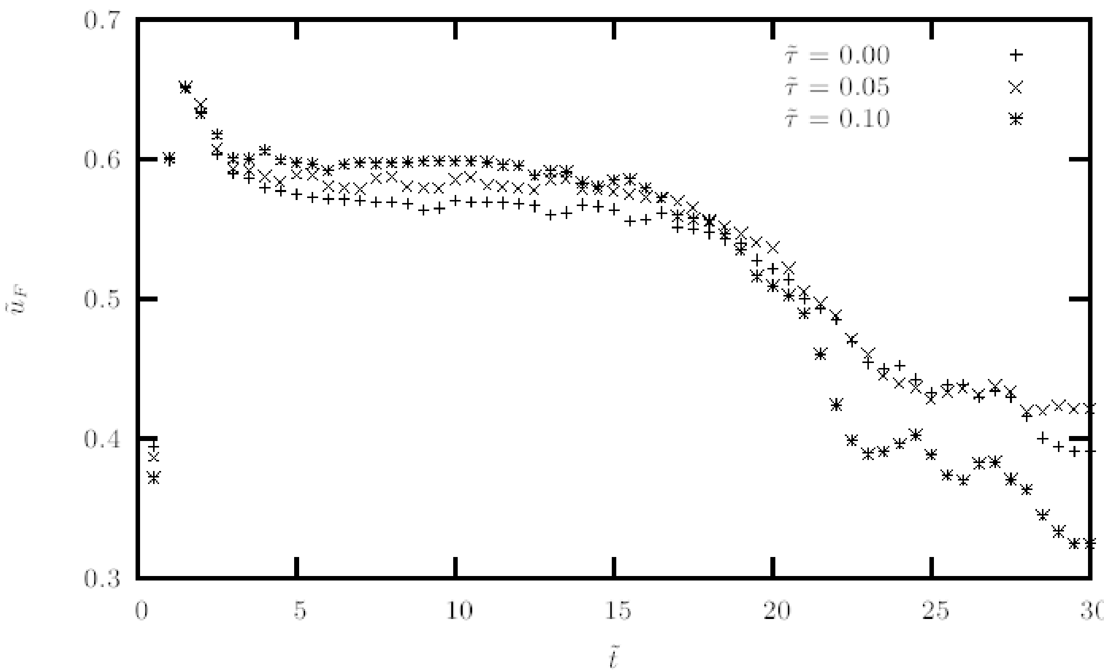

FIGURE 10. ***Front velocity of gravity currents for total time of simulation. Solution for w=0 and Gr=1.5 x 10^6.***